MJFAS MALAYSIAN JOURNAL OF FUNDAMENTAL AND APPLIED SCIENCES
PRINT ISSN: 2289-5981 | ONLINE ISSN: 2289-599X

RESEARCH ARTICLE

A comparison of degradation rate bone scaffold morphology between computer simulation and experimental approach

Akbar Teguh Prakoso [a], Ardiyansyah Syahrom [b,c], Mohd Ayub Sulong [b,c], Amir Putra Md. Saad [b], Irsyadi Yani [a], Jimmy Deswidawansyah Nasution [a], Hasan Basri [a,*]

[a] *Department of Mechanical Engineering, Faculty of Engineering, Universitas Sriwijaya, Inderalaya 30662, Kabupaten Ogan Ilir, Indonesia*
[b] *Department of Applied Mechanics and Design, Faculty of Mechanical Engineering, Universiti Teknologi Malaysia, Skudai 81310, Johor, Malaysia*
[c] *Sports Innovation and Technology Centre (SITC), Institute of Human-Centred and Engineering (IHCE), Universiti Teknologi Malaysia, Skudai 81310, Johor, Malaysia*

* *Corresponding author: hasan_basri@unsri.ac.id*

Article history
Received 15 October 2017
Accepted 6 December 2017

Abstract

The aim of this research is to validate the behavior of degradation rate within porous magnesium scaffolds in terms of morphological which includes weight loss after degradation by way of micro-computed tomography (µCT) based on image processing. The main contribution of this work is finding another method to determine morphology based on computer simulation. In the present work, bone scaffold specimens made of pure magnesium that was set up with three different percentages of porosities 30%, 41%, and 55%. There were immersed and subjected to the dynamic flow rate of simulated body fluid for periods of 24, 48 and 72 hours. One sample of each specimen was scanned by µCT with a resolution of 17 µm. The cross-segments of raw data were laid over by using MIMICS software to make a 3D reconstruction of the samples after degradation. The degradation morphology was collected from the simulation and showed good agreement with the experimental results by only less than 2%. Based on the simulation results, it is possible to give a recommendation for the alternative way in the morphological study of orthopedic applications.

Keywords: Degradation rate, Bone scaffold, Morphology, Image processing

INTRODUCTION

The most successful strategies in tissue engineering scaffold required that the morphological, micro-architectural, mechanical properties and biodegradation behavior feature well tolerated by the host tissue matching the targeted clinical application in healthcare [1]. It is commonly recognized that morphology actively influences the biological fluids and oxygen transport for their maintenance and subsequently, influencing the in vivo conductive response of the structure after its implantation [2-4]. As a consequence, the degradation properties of scaffolds are relevant both to the biomaterial design and to the long-term success of a tissue engineering structure. Bone tissue engineering scaffold as the biodegradable metals aims to overcome the drawbacks of the current bone regeneration techniques in orthopedic applications. Degradation assessment systems of biodegradable metals must be carefully considered for the specific applications. Therefore, biodegradable material selection must be performed because the material must have a good balance between mechanical properties and degradation behavior. Scaffolds must possess enough mechanical properties matching that of the cancellous bone and strength must be maintained for an adequate period of time, despite the ongoing degradation of the implant, which will ultimately lead to scaffold resorption and loss of mass. In the previous work [5,6] determined the degradation rate of the porous magnesium specimens that was worked out based on weight loss measurement method and hydrogen development.

Micro-computed tomography (µCT) is a technique that can be applied to analyze the cancellous and cortical bone microarchitecture in microscale [7]. Microarchitectural analysis of cancellous bone using µCT has been investigated by Müller, R. *et al*. [8-11]. Thus, on that point is a clear potential for µCT techniques to estimate the morphology of tissue engineering bone scaffold in 3D. This paper describes the image processing and three-dimensional visualization of bone scaffold degradation morphology to measure the mass remaining, volume, and weight loss after 72 hours immersion period.

The aim of this research was to examine an image processing method for determination of mass remaining and weight loss of bone scaffolds. The method provides a valuable alternative to the conventional methods for measurement of weight loss of bone scaffold and can be used to evaluate the bone morphology of medical interest due to the clinical importance of tissue replacement.

In the future, the three-dimensional model based on image processing allows one to investigate the potential connectivity between the host bone and the bone ingrowth within the scaffold.

MATERIALS AND METHOD

Scaffold preparation and characterization

Cuboid-shaped (5×5×3 mm) of commercially available pure magnesium with a rod diameter of 24.4 mm and 99.9% purity (made by Good Fellow Inc, Cambridge, UK) having interconnected holes which were fabricated using CNC machine (HAAS, USA) [5,6]. The samples were drilled using a drill bit of 800 µm in diameter. The porous magnesium of bone scaffold with varying porosity and surface area can

be exhibited in Fig. 1. The morphological indices of the specimens, including porosity, surface area, volume, the surface area per volume were determined using CAD models [28] and are shown in Table 1.

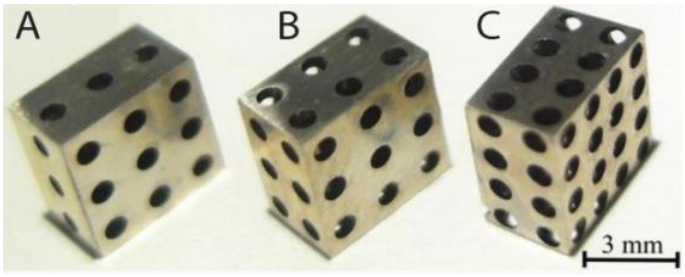

Fig. 1. Snapshots of three different morphologies of bone scaffold specimens [5,6].

Table 1. The morphological details of the bone scaffold specimens [5,6].

Type	Porosity	Surface Area	Volume	Surface area per volume
A	30%	189.30 mm^2	52.87 mm^3	3580.48 m^{-1}
B	41%	209.81 mm^2	44.57 mm^3	4704.43 m^{-1}
C	55%	225.75 mm^2	33.83 mm^3	6673.07 m^{-1}

Three groups of specimens with different morphologies were labeled as sample *A*, *B*, and *C*. The samples were made with three different porosities 30%, 41%, and 55%, respectively, which were led on the basis of the morphology of cancellous bone [12,13]. On the other hand, in vitro experimental model were conducted to translate the bone marrow through a cancellous bone.

Simulated body fluid was prepared to represent the bone. The porous magnesium specimens were subjected to dynamic immersion tests using the test rig system using an SBF as per Kokubo *et al*. [33] that has a composition per liter as shown in Table 2. The pH of the SBF was adjusted to 7.4 using drops of 1.0 M HCl of up to 5 ml, and its temperature was maintained at $37^0C \pm 1^0C$; the flow rate was kept constant at 0.025 ml/min. The specimens were then subjected to dynamic immersion tests for periods of 24h, 48h, and 72 h. The SBF volume used in this study was 250 ml. The same volume was re-circulated through particular dynamic immersion test periods [5,6].

Table 2. Order and amount of composition, preparation for 1 liter SBF solution [5,6].

Order	Reagent	Quantity
1	NaCl	8.035 g
2	$NaHCO_3$	0.355 g
3	KCl	0.225 g
4	$K_2HPO_4.3H_2O$	0.231 g
5	$MgCl_2.6H_2O$	0.311 g
6	HCl1.0M	39 ml
7	$CaCl_2$	0.292 g
8	Na_2SO_4	0.072 g
9	Tris buffer	6.118 g
10	HCl 1.0M	1-5 ml

The degradation rate was determined to use the weight loss measurement method [5,14]. A diluted acid solution (H2CrO4) was employed to carry away the degradation products on the surface of the tested specimens. The weight loss and porosities for each dynamic test with a different time of immersions was evaluated by using Eq. (1) and Eq. (2).

$$\Delta W_{\%\ degradation\ rate} = [(W_i - W_o) / W_i] \times 100 \quad (1)$$

$$(\%)\ Porosity = [(W_i - W_o) / \rho V_1] \times 100 \quad (2)$$

where W_i and W_o are the weight of specimen before and after immersion in SBF, respectively, ρ is the density of magnesium and V_1 is the volume before immersion in SBF. Weight loss of bone scaffold degradation was measured and compared to its original weight. For example, 20% weight loss means 80% of the original weight of scaffold remains in the bulky scaffolds, for 100% biodegradation indicates the complete collapse of the scaffold [15].

Micro-computed tomography (μCT) evaluation

In order to validate degradation rate bone scaffold morphologies, one sample from each porosity (i.e. *A*, *B* and *C*) and each immersion group (i.e. *24h*, *48h*, and *72h*) were scanned by means of micro-computed tomography device. For simulation purposes, there only 9 samples were scanned in the Simulated body fluid. Fig. 3 shows a reconstructed model of 9 immersed samples, from sample *A = 24h* to *C = 72h*. Raw images with a resolution of 17.20 μm by using a μCT scanner (Skycan 1172, Kontich, Belgium) were taken. The μCT technique has been utilized in tissue engineering with the purpose to assess the tissue integration, tissue formation and scaffold degradation [16]. In general, μCT datasets provide spatial information, suitable for measurements of various bone parameters such as bone volume, bone thickness and bone mineral density [17].

Image segmentation and reconstruction

The process to obtain a three-dimensional model from raw μCT images of the bone scaffold is illustrated step-by-step process as shown in Fig. 2. Representative cross-sectional images of the specimen after degradation is shown in Fig 2a. The data from μCT scan was processed by using the so-called gray value thresholding. The most important part of this step is to differentiate between the solid phase (i.e. specimen) from the air. After that, the raw data images are transformed into a binary form or simply black and white voxel and the scale of images have been set up with the true scale. The white voxel in the micrograph is grouped into the solid phase while a black voxel represents the air. Segmentation or thresholding procedure is taken by using ImageJ software commands to determine the proper value of grayscale [18]. ImageJ provides global thresholding algorithms by means of the plugin named Auto Threshold [19-24]. In this subject field, automatic thresholding algorithm based on the Otsu's method was available in ImageJ is the best method to demonstrate good correspondence with the interactive method performed by consultant [23-27]. The raw threshold images data has been shown in Fig.2b and saved in (8-bit TIFF) format images [28]. Finally, the raw data images after segmentation were exported into commercially available software (MIMICS; materialize, Louvain, Belgium) and the three-dimensional volume rendering can be generated with the 3D mask calculate using a software command (see Fig. 2c) on the workstation running 64-bit Windows XP Professional with an Intel Pentium i7 and 128 GB of RAM.

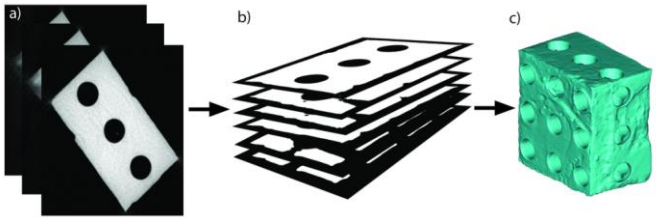

Fig. 2. Representative of the preparation procedure of bone scaffold reconstruction: a) Raw data μCT, b) Segmentation of image stacks and c) 3D model reconstruction.

Basically, there are several approaches to the design of the 3D model, include a CAD-based method, image base design, implicit surfaces and space-filling curves [29]. Images-base modeling is the preferred method to provides high quality, more accurate and reliable quantitive 3D data [30]. By using MIMICS command, the volume of

virtual models has been obtained and the mass model is calculated by multiplying the 3D model volume by the Mg material density, as shown in Eq. (3).

$$Mass = V \times \rho \quad (3)$$

where ρ is the density of the pure Mg (1.74 g/cm^3) [31].

RESULTS AND DISCUSSION

Degradation morphology

From the raw data set of tomographic images, a three-dimensional reconstruction of bone scaffolds efficiently approximates the real surface which has been generated. Comparability of the morphology of each specimen between the simulation and experimental results is presented in Fig. 3. The investigation of the three-dimensional structure leads to further inform the process of implant degraded. A 3D reconstruction of µCT slices using MIMICS allowed a qualitative appraisal of the pore interconnectivity within the replica scaffolds.

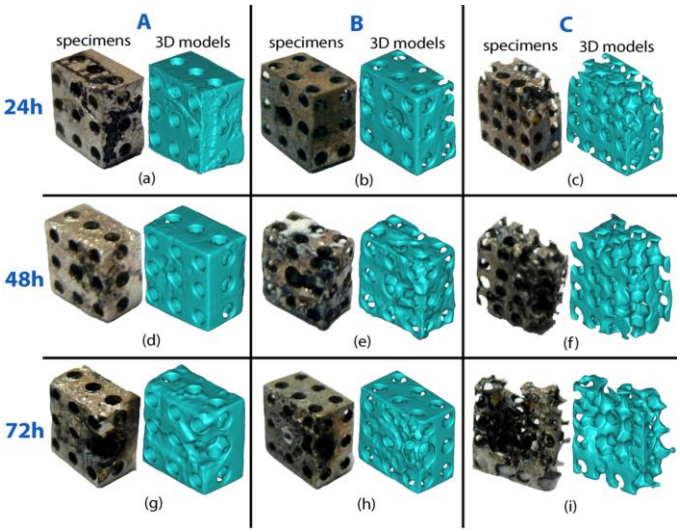

Fig. 3. Photograph of the comparative morphology between samples and 3D reconstructed models of bone scaffold after biodegradation.

Simulation results

The comparison between experimental and simulation results of weight remaining during biodegradation are shown in Table 3. The results showed better agreement with an error less than 2%. The lower of percentage error mean that the closer the simulation results are in the experimental results.

Table 3. The comparison of bone scaffold weight remaining between experiment and simulation results.

Sample	Periodic immersion (hours)	Weight remaining (%)		% Error
		Experimental	Simulation	
A	24	88.949	89.855	1.010
	48	87.331	88.647	1.485
	72	83.816	85.481	1.947
B	24	86.671	86.828	0.180
	48	78.478	80.142	2.076
	72	78.037	78.620	0.742
C	24	78.912	79.925	1.268
	48	62.946	63.902	1.500
	72	58.705	59.437	1.231

Scaffold evaluation

In vitro and simulation biodegradation behavior of magnesium scaffolds (i.e. the percentage of weight loss) was evaluated in SBF for 72 hours and the results are shown in Fig. 4. The results indicate that the scaffold was biodegradable and the degradation of scaffolds was gradually increased over the compactness time. The model's simulation matched the experimental data reasonably well during all immersion periods. As can be understood, the degradation of pure magnesium scaffold was relatively faster than that of the other groups. Sample *C* showed a 20% weight loss at *24* hours, but sample A and *B* showed about 10% and 13% weight loss, which indicated that the presence of the porosity significantly enhances the biodegradation rate of the bone scaffolds.

Furthermore, the percentage weight loss of the whole samples after 48 hours of immersion lower than before. For illustration, the increment weight loss from 48 to 72 hours for A, B, and C samples are 3.5, 1.8, and 4.4% respectively. These results can probably be attributed to the presence of hydrogen gas evolution, which are difficult to remove from the surface of the scaffold [5,32]. This may also explain why the biodegradation rate of the scaffold was slower at 72 hours immersion.

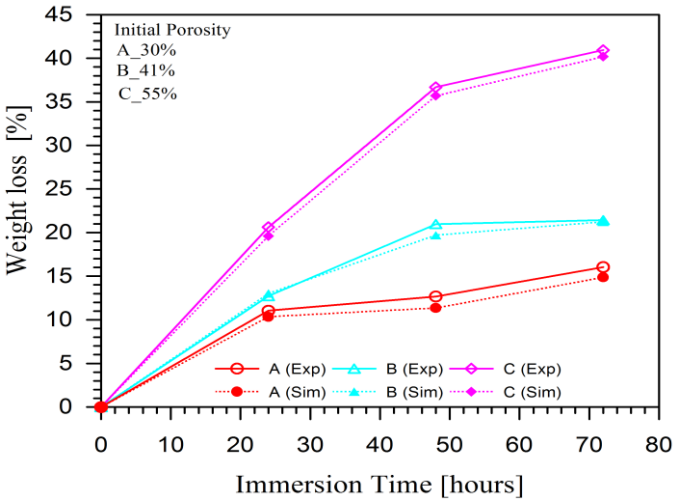

Fig. 4. The comparison of the weight loss of bone scaffold after biodegradation between experiment and simulation results.

CONCLUSION

In this research, the degradation rate of bone scaffold morphology after degradation has been successfully developed by applying computer simulation based on image processing. The simulation results showed good agreement with the experimental results by just less than 2%. The biodegradation behavior of bone scaffold gradually increased under the immersion time and then the presence of the porosity significantly enhances the biodegradation rate of the bone scaffolds.

In the future, the computer simulation based on image processing is brought out to develop a three-dimensional model and it can be easily converted to STL format to analyze mechanobiology of bone scaffolds using finite element analysis and to achieve a three-dimensional printing in biomedical applications.

ACKNOWLEDGEMENT

This study was part of an International Research Collaboration between Universitas Sriwijaya, Indonesia and the Universiti Teknologi Malaysia, Malaysia.

REFERENCES

[1] F. J. O'Brien, 2011. Biomaterials and scaffolds for tissue engineering. *Material Today* 14(3), 88–95.

[2] G. Ciapetti, L. Ambrosio, G. Marletta, N. Baldini, and A. Giunti, 2006. Humanbone marrow stromal cells: In vitro expansion and differentiation for bone engineering. *Biomaterials* 27, 6150–6160.

[3] V. Guarino, F. Causa, and L. Ambrosio, 2007. Bioactive scaffolds for bone and ligament tissue. *Expert Review of Medical Devices* 4(3), 405–418.

[4] L. Savarino, N. Baldini, M. Greco, O. Capitani, S. Pinna, S. Valentini, B. Lombardo, M.T. Esposito, L. Pastore, L. Ambrosio, S. Battista, F. Causa, S. Zeppetelli, V. Guarino, P.A. Netti, 2007. The performance of poly-ε-caprolactone scaffolds in a rabbit femur model with and without autologous stromal cells and BMP4. *Biomaterials* 28(20), 3101–3109.

[5] Amir Putra Md. Saad, Noor Jasmawati, Muhamad Noor Harun, Mohammed Rafiq Abdul Kadir, Hadi Nur, Hendra Hermawan, and Ardiyansyah Syahrom, 2016. Dynamic degradation of porous magnesium under a simulated environment of human cancellous bone. *Corrosion Science* 112, 1-12.

[6] Amir Putra Md. Saad, Rabiatul Adibah Abdul Rahim, Muhamad Noor Harun, Hasan Basri, Jaafar Abdullah, Mohammed Rafiq Abdul Kadir, and Ardiyansyah Syahrom, 2017. The Influence of flowrates on the dynamic degradation behavior of porous magnesium under a simulated environment of human cancellous bone. *Materials & Design* 122, 268-279.

[7] A. C. Jones, Bruce Milthorpe, Holger Averdunk, Ajay Limaye, Tim J. Senden, Arthur Sakellariou, Adrian P. Sheppard, Rob M. Sok, Mark A. Knackstedt, Arthur Brandwood, Dennis Rohner, Dietmar W. Hutmacher, 2004. Analysis of 3D bone ingrowth into polymer scaffolds via micro-computed tomography imaging. *Biomaterials* 25(20), 4947–4954.

[8] R. Muller, T. Hildebrand, and P. Ruegsegger, 1994. Non-invasive bone biopsy: a new method to analyze and display the three-dimensional structure of trabecular bone. *Physics in Medicine and Biology* 39(1), 145-164.

[9] R. Muller, M. Hahn, M. Vogel, G. Delling, and P. Ruegsegger, 1996. Morphometric analysis of noninvasively assessed bone biopsies: comparison of high-resolution computed tomography and histologic sections. *Bone* 18(3), 215-220.

[10] J. R. Vetsch, R. Müller, and S. Hofmann, 2015. The evolution of simulation techniques for dynamic bone tissue engineering in bioreactors. *Journal of Tissue Engineering and Regenerative Medicine* 9(8), 903–917.

[11] G. H. Van Lenthe, H. Hagenmüller, M. Bohner, S. J. Hollister, L. Meinel, and R. Müller, 2007. Nondestructive micro-computed tomography for biological imaging and quantification of scaffold-bone interaction in vivo. *Biomaterials* 28(15), 2479–2490.

[12] L. Polo-Corrales, M. Latorre-Esteves, and J. E. Ramirez-Vick, 2014. Scaffold design for bone regeneration. *Journal of Nanoscience and Nanotechnology* 14(1), 15–56.

[13] K. G. Prashanth, K. Zhuravleva, I. Okulov, M. Calin, J. Eckert, and A. Gebert, 2016. Mechanical and corrosion behavior of new generation Ti-45Nb porous alloys implant devices. *Technologies* 4(33), 1-12.

[14] M. Zhao, P. Schmutz, S. Brunner, M. Liu, G. Song, and A. Atrens, 2009. An exploratory study of the corrosion of Mg alloys during interrupted salt spray testing. *Corrosion Science* 51(6), 1277–1292.

[15] A. Shahini, M. Yazdimamaghani, K. J. Walker, M. A. Eastman, H.H. Marbini, B. J. Smith, J. L. Ricci, S.V. Madihally, D. Vashaee, and L. Tayebi, 2014. 3D conductive nanocomposite scaffold for bone tissue engineering. *International Journal of Nanomedicine* 9, 167–181.

[16] A. Papadimitropoulos, M. Mastrogiacomo, F. Peyrin, E. Molinari, V.S. Komlev, F. Rustichelli, and R. Cancedda, 2007. Kinetics of in vivo bone deposition by bone marrow stromal cells within a resorbable porous calcium phosphate Scaffold: An X-ray computed microtomography study. *Biotechnology and Bioengineering* 98(1), 271–281.

[17] Martin Baiker, Thomas J. A. Snoeks, Eric L. Kaijzel, I. Que, J. Dijkstra, Boudewijn P. F. Lelieveldt, Clemens W. G. M. Löwik, 2012. Automated bone volume and thickness measurements in small animal whole-body MicroCT data. *Molecular Imaging and Biology* 14(4), 420–430.

[18] P.J. Reynisson, M. Scali, E. Smistad, E.F. Hofstad, H.O. Leira, F. Lindseth, Toril A.N. Hernes, T. Amundsen, H. Sorger, and T. Langø, 2015. Airway segmentation and centerline extraction from thoracic CT - Comparison of a new method to state of the art commercialized methods. *PLoS One* 10(12), 1–20.

[19] Y. Zhang, Z. He, S. Fan, K. He, and C. Li, 2008. Automatic thresholding of micro-CT trabecular bone images. *BMEI '08 Proceedings of the 2008 International Conference on Biomedical Engineering and Informatics* 2, 23-27.

[20] M. Doube, M.M. Kłosowski, I.A. Carreras, F.P. Cordelières, R.P. Dougherty, J. S. Jackson, B. Schmid, J.R. Hutchinson, and S.J. Shefelbine, 2010. BoneJ: Free and extensible bone image analysis in ImageJ. *Bone* 47, 1076–1079.

[21] C. Science, 2017. Automatic thresholding from the gradients of region boundaries. *Journal of Microscopy* 265(2), 185–195.

[22] R. Geesala, N. Bar, N. R. Dhoke, P. Basak, and A. Das, 2016. Data on bone marrow stem cells delivery using porous polymer scaffold. *Data in Brief* 6, 221–228.

[23] M. A. Alkubeyyer, H. Al-Khodair, and S. Alsultan, 2013. Comparisons of interactive and multiple automated methods for mammographic density index quantification. *Poster presented at European Congress of Radiology*, ECR 2013, C-0359, 1-11.

[24] E. Sales, I. Lima, J.T. de Assis, W. Go´mez, W. C. A. Pereira, and R. T. Lopes, 2012. Bone quality analysis using X-ray microtomography and microfluorescence. *Applied Radiation and Isotopes* 70(7), 1272–1276.

[25] W. Van Aarle, K. J. Batenburg, and J. Sijbers, 2011. Optimal threshold selection for segmentation of dense homogeneous objects in tomographic reconstructions. IEEE *Transactions on Medical Imaging* 30(4),980-989.

[26] P. Sharma, A. Joshua, and M. Singh, 2013. A novel approach towards x-ray bone image segmentation using discrete step algorithm. *International Journal of Emerging Trends & Technology in Computer Science* 2(5), 191–195.

[27] M. Rekha and A. Meera, 2013. Tumor detection using K-Mean clustering algorithm method. *International Journal of Scientific & Engineering Research* 4(8), 2226-2230.

[28] E. Descamps, A. Sochacka, B. De Kegel, D. Van Loo, L. Van Hoorebeke, and D. Adriaens, 2014. Soft tissue discrimination with contrast agents using micro-CT scanning. *Belgian Journal of Zoology* 144(1), 20–40.

[29] Z. Larimore, S. Jensen, P. Parsons, B. Good, K. Smith, and M. Mirotznik, 2017. Use of space-filling curves for additive manufacturing of three-dimensionally varying graded dielectric structures using fused deposition modeling. *Additive Manufacturing* 15, 48-56.

[30] T. A. Alam, Q. L. Pham, V. I. Sikavitsas, D. V. Papavassiliou, R. L. Shambaugh, and R. S. Voronov, 2016. Image-based modeling: A novel tool for realistic simulations of artificial bone cultures. *Technology* 4(4), 229-233.

[31] M. A. Sulong, V. Mathier, T. Fiedler, I. V. Belova, and G. E. Murch, 2014. Compressive properties of Corevo® foam under uni-axial loading based on the experimental and numerical analysis. *Applied Mechanics and Materials* 597, 121–126.

[32] N. Ishida Zainal Abidin, B. Rolfe, H. Owen, J. Malisano, D. Martin, J. Hofstetter, P. J. Uggowitzer, and A. Atrens, 2013. The in vivo and in vitro corrosion of high-purity magnesium and magnesium alloys WZ21 and AZ91. *Corrosion Science* 75, 354–366.

[33] T. Kokubo, H. Takadama, 2006. How useful is SBF in predicting in vivo bone bioactivity? *Biomaterials* 27, 2907–2915.